Design of Blends with an Extremely Low Viscosity Ratio between the Dispersed and Continuous Phases. Dependence of the Dispersed Phase Size on the Processing Parameters

Jonathan Leblanc,[1] *Mathilde Mercier,*[2] *Christian Fonteix,*[1] *Fernand Pla**[1]

Summary: This work deals with the development of the dispersed phase morphology in immiscible blends of poly(ethylene glycol)/polyamide 66 (PEG/PA) with an extremely low viscosity ratio. The blends were obtained, under different operating conditions, by melt blending in an internal mixer. The objective was to examine the influence of the main processing parameters on the particles size of the minor phase (PEG). A model was elaborated to describe the dependence of the particle size on interfacial tension, PEG concentration, shear rate and viscosity ratio between the two blend components.

Keywords: blends; modeling; morphology; processing parameters

Introduction

Most of useful polymer blends are elaborated with immiscible polymers, leading to a multiphase morphology from which most properties of the blend are strongly dependent. So, it is particularly important to control the processing parameters, which are able to affect this morphology. Numerous studies, focused on binary blends with a viscosity ratio comprised between 0.01 and 20, have been performed in this way. For example, Wu[1] proposed a correlation between the number average diameter of the dispersed phase, (d_n), the shear rate, ($\dot{\gamma}$), the ratio, (p), of the viscosity of the dispersed phase (η_d) over that of the matrix (η_m) and the interfacial tension (γ):

$$\frac{\dot{\gamma}\eta_m d_n}{\gamma} = 4(p)^{\pm 0.84} \quad (1)$$

In this equation, the exponent is positive when p is higher than 1 and negative when p is lower than 1. Serpe and al.[2] modified this equation in order to also take into account the effect of the concentration of the dispersed phase. They replaced the viscosity of the matrix by the viscosity of the blend (η_b) and introduced the following empirical function:

$$F(\phi) = 1 - (4\phi_d\phi_m)^{0.8} \quad (2)$$

where φ_d and φ_m are the volume fraction of the dispersed phase and the matrix respectively. Finally they obtained the relationship:

$$\frac{\dot{\gamma}\eta_b d_n F(\phi)}{\gamma} = 4\left(\frac{\eta_d}{\eta_b}\right)^{\pm 0.84} \quad (3)$$

In this work, the case of Poly(ethylene glycol)/Polyamide 66 (PEG/PA 66) blends with an extremely low viscosity ratio will be examined. First, a protocol will be established to elaborate these blends using an internal mixer with a conical chamber. In a second step, a correlation between the shear rate and the rotors speed of this equipment will be proposed. Then, the influence of PEG concentration and shear rate on the

[1] Laboratoire des Sciences du Génie Chimique/CNRS/Nancy université, 1 rue Grandville, BP 20451, F-54001 Nancy Cedex, France
E-mail: fernand.pla@ensic.inpl-nancy.fr
[2] Rhodia Recherches & Technologies – CRTL, Groupe Polymères, 85 rue des Frères Perret, BP 62, F-69192 Saint-Fons Cedex, France

morphology of the resulting blends will be analyzed. This will lead to the establishment of a correlation between the dispersed phase size and the processing parameters.

Experimental Part

Materials

Polyamide 66 (from Rhodia) was used as matrix and a poly(ethylene glycol) (from Aldrich) as dispersed phase.

Silicone oil (from Rhodia Silicone) was used as a calibration fluid to determine the shear rate in the mixer.

2,2,2–Trifluoroethanol (TFE), Chloroform-D ($CDCl_3$) and Dichloromethane (CH_2Cl_2) were purchased from Sigma-Aldrich.

Protocol for the Elaboration of the Blends

Blends were prepared at 275 °C in a Haake internal mixer (Rheomix 540p), equipped with two roller blade rotors. Prior to mixing, PA and PEG were dried, respectively at 80 °C and 40 °C, under vacuum overnight. A series of preliminary thermogravimetric analyses clearly showed a degradation of PEG at 275 °C under air atmosphere, while the product kept its chemical integrity under inert conditions. For this reason, all experiments were carried out under nitrogen atmosphere. PA was first melted in the mixing chamber for 5 min. at 200 rpm. Then, the rotors speed was reset to the desired value for the run and PEG was introduced in the chamber. After 5 min., the rotors were stopped and a sample of the blend was quenched in liquid nitrogen.

Operating conditions of all runs are reported in Table 1. The rotors speed was varied between 100 and 200 rpm. The feeding PEG weight fraction was set between 1 and 20%. During the PEG introduction, a small amount of the product adhered to the walls of the vessel containing it. The accurate values of the feeding PEG weight fraction were obtained from the difference of the vessel mass before and after each PEG introduction. The value of the mixing time given in this table corresponds to the time elapsed between the introduction of PEG in the mixing chamber and the rotors stop. The filling ratio is the ratio between the volume of the materials at the mixing temperature and the volume of the chamber. Seven runs were carried out according to the protocol described above. Run 8 corresponds to the duplication of run 3.

Complementary runs were also performed in order to evaluate the influence of the protocol addition (run 9 for which PEG and PA were introduced simultaneously in the mixing chamber), the mixing time (run 10) and the filling ratio (run 11).

Analytical Techniques

Viscosity

The viscosity of PEG, measured on a dynamic stress rheometer, showed a Newtonian behavior with a viscosity of 4.10^{-3}

Table 1.
Operating conditions used for the elaboration of the blends.

	Number	Rotors speed (rpm)	(PEG/PA) (%)	Addition protocol	Mixing time (min)	Filling ratio
Main experiments	1	200	1/99	Sequential	5	0,69
	2	200	10/90	Sequential	5	0,68
	3	200	20/80	Sequential	5	0,79
	4	150	20/80	Sequential	5	0,78
	5	100	1/99	Sequential	5	0,69
	6	100	10/90	Sequential	5	0,68
	7	100	20/80	Sequential	5	0,77
	8	200	20/80	Sequential	5	0,78
Complementary experiments	9	200	20/80	Simultaneous	5	0,78
	10	200	20/80	Sequential	10	0,77
	11	200	1/99	Sequential	5	0,79

Pa · s at 275 °C. The viscosities of the PA were 224.5 Pa · s and 203.8 Pa · s for 10 and 100 s^{-1} respectively (data from suppliers). So the viscosity ratio of the two blend components was about 1.9×10^{-5}.

Morphology

The blends morphology was examined by using a JEOL JSM-T330A scanning electron microscope (SEM). Before observations, the samples were held in liquid nitrogen, cryo-fractured and immersed in boiling dichloromethane overnight to remove the dispersed phase (PEG). They were then dried and their surface was coated with gold to make them conductive. An image analysis software (Image tools 3.0) was used to measure the areas of the PEG particles observed on the micrograph. These areas were then converted to particle diameters, d_i.

When the size distribution was too large to view all the particles through only one magnification, the measurements were performed at two different magnifications. The global distribution was obtained by combining the two frequency histograms. This was made by scaling the two histograms in proportion to the reference area of the images used at each magnification. The average diameters d_{10} and d_{21} were then deduced from the two following equations:

$$d_{10} = \frac{\sum N_i d_i}{\sum N_i} \quad (4)$$

$$d_{21} = \frac{\sum N_i d_i^2}{\sum N_i d_i} \quad (5)$$

where N_i and d_i are the number and the diameter of the *i*th domain respectively.

Blends Composition

The actual concentration of PEG in blends was measured by 1H N.M.R spectroscopy. A sample was dissolved in a mixture of (TFE/$CDCl_3$) (50/50). Measurements were performed on a Brucker 300 MHz (model Avance 300) spectrometer. The relative proportion of PEG was established by integrating specific peaks of the two polymers. The peaks at 3.65–3.3 ppm correspond to the PEG hydrogen atoms while those at 1.78–1.25 ppm correspond to polyamide hydrogen atoms. It was necessary to remove the integral value of TFE satellites, specifically measured at 4.12–3.96 ppm, from that corresponding to PEG.

Results and Discussion

Shear Rate in the Mixer

The main difficulty to determine the shear rate from mixer data comes from the complex flow in the mixer, generated by the geometry of the rotors.

To overcome this issue, Goodrich and Porter[3] considered the internal mixer as two adjacent sets of concentric cylinders (Couette analogy) and calculated the shear rate from the external (R_e) and internal (R_i), radii of the model mixer.

Bousmina and al.[4] validated this approach and proposed a general procedure to estimate the shear rate. In their study, Re is equal to the radius of the mixing chamber and R_i is obtained through a calibration procedure with a fluid for which the viscosity-shear rate dependence is known. Hence, Bousmina and al.[4] established a relationship to calculate the internal radius knowing the rheological characteristics of the fluid and the torque, (Γ), in the mixer at the equilibrium:

$$R_i = \frac{R_e}{\left[1 + \frac{4\pi N}{n}\left(2\pi M L R_e^2 \frac{1+g^{n+1}}{\Gamma}\right)^{\frac{1}{n}}\right]^{\frac{2}{n}}} \quad (6)$$

where N is the rotor speed, M the polymer melt consistency, n the power law index, g the gear ratio between the two rotors ($g = 2/3$), L the length of the rotor.

The authors proved that, for a given type of mixer, the value of R_i is independent of the nature of the fluid. This work was completed by the study of Ait-Kadi and al.[5] who showed that, for a ratio R_i/R_e higher than 0.7, there is a position in the gap between the two concentric cylinders where the shear rate is almost independent of the nature of the fluid: the error on the shear rate is ±10% by considering the Newtonian approach at this position. This optimal

position is given by:

$$r* = \left[\frac{n'}{n} \times \frac{\left(\frac{R_e}{R_i}\right)^{\frac{2}{n'}} - 1}{\left(\frac{R_e}{R_i}\right)^{\frac{2}{n}} - 1} \times R_e^{\left(\frac{2}{n} - \frac{2}{n'}\right)} \right]^{\frac{1}{\frac{2}{n} - \frac{2}{n'}}} \quad (7)$$

where n and n' are two flow behaviour indices representative of the range of shear-thinning fluids to be studied (generally, $n = 0.15$ and $n' = 1$). At this position, the shear rate is:

$$\gamma = \frac{4\pi N}{n} \frac{\left(\frac{R_e}{r*}\right)^{2/n}}{\left(\frac{R_e}{R_i}\right)^{2/n} - 1} \quad (8)$$

In the case of the Haake Rheomix 540p, the mixing chamber is conical and the radius of the chamber varies from 20 mm to 22,5 mm. Nevertheless, the Couette analogy was applied to this system by assuming that the external radius, Re, was equal to the mean radius (21.25 mm). The calibration procedure was performed using silicone oil because this fluid can be used for temperatures near to ambient at which degradation problems are negligible. Nevertheless, some difficulties were encountered measuring the steady-shear viscosity of the oil in the usual range of shear rate used in internal mixers (10–100 s^{-1}) because below a shear rate of 2.5 s^{-1} a fraction of oil was evicted from the plates. Nevertheless, as shown in Figure 1, below 2.5 s^{-1}, the shear viscosity of the oil, η, was practically equal to the dynamic viscosity. So the Cox – Merz' rule was checked out for low shear rates and it was assumed that it was also valid for the high shear rates.

Consequently, dynamic measurements were used to represent the rheological behaviour of the oil. As shown in Figure 1, for shear rates between 10 s^{-1} and 100 s^{-1}, the following power law, allowing fitting the viscosity, was obtained:

$$\eta = 886\dot{\gamma}^{-0.33} \quad (9)$$

Table 2, shows that the values of R_i, calculated under different processing conditions using equation (6), are practically constant. Its mean value (15.95 mm) was used to determine, owing to equation (7), the optimal position, r^*, (17.56 mm), for which R_i/R_e is higher than 0.7. The corresponding shear rate deduced from equation (8) by using a Newtonian approach ($n = 1$) is:

$$\dot{\gamma} = 23.74N \quad (10)$$

where N is expressed in round per second.

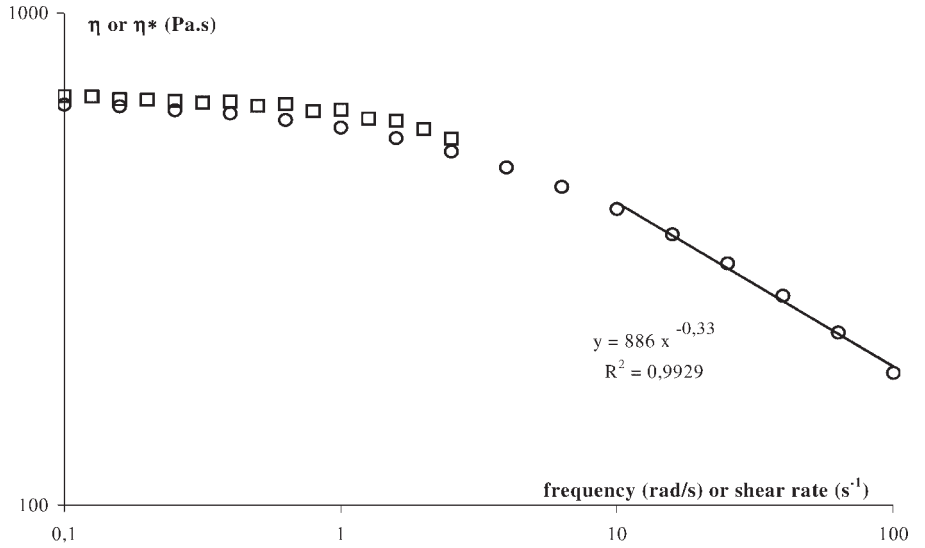

Figure 1.
Comparison between the dynamic viscosity (○) and the steady shear viscosity (□) of the silicone oil.

Table 2.
Internal radius determined under different processing conditions.

Rotor speed (rpm)	T (°C)	Γ (Nm)	R_i (mm)
100	35	1.43	15.85
120	35	1.7	16.09
150	35	2.02	16.19
180	35	1.97	15.51
200	35	2.42	16.14

To know the error made on the shear rate by considering a mean external radius for the conical chamber, the same procedure was applied for its extreme values (20 mm and 22,5 mm). It shows a difference of ±10% on the corresponding shear rates.

Incorporation Rate

Figure 2 allows comparing PEG concentrations in the blends, Cm, (determined by ^{1}H N.M.R spectroscopy), with that of PEG introduced in the mixer, Ci. The proportionality coefficient between these two quantities (called incorporation rate, Y), is equal to 0.95. To see if this coefficient is representative of all experiments, a 10% confidence interval for experimental data was calculated using Student's distribution:

$$\hat{C} - Stu_{0.95}\sqrt{\sigma_g^2} \leq C_m \leq \hat{C} + Stu_{0.95}\sqrt{\sigma_g^2} \tag{11}$$

where $\hat{C}$ is the PEG weight percentage estimated by the product (Ci).(Y), $Stu_{0.95}$ is the value of the Student criterion at 5% and σ_g^2 is the global error variance

Figure 2 shows that almost all main experiments are within this interval. This allowed considering that the value of the incorporation rate can be applied for all runs.

In the case of the simultaneous addition of PEG and PA, Figure 2 shows that the representative point is below the lower limit of the confidence interval indicating that the incorporation rate is lower in this case. That's why, in the protocol, the two blend components were introduced sequentially rather than simultaneously.

Runs 10 and 11 are within the interval confidence: a change on filling ratio (from 0.7 to 0.8) as well as on mixing time (from

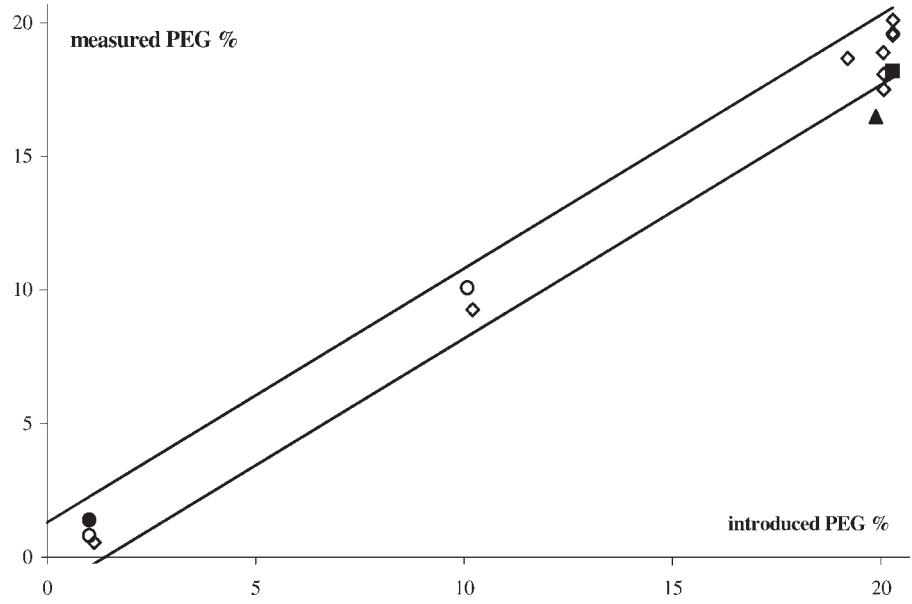

Figure 2.
Comparison between introduced and measured PEG concentration in blends; ◇ = main experiments, ▲ = effect of protocol addition (run 9), ■ = effect of mixing time (run 10), ● = effect of filling ratio (run 11).

5 to 10 minutes) appeared to have no influence on the incorporation rate.

Morphology

Reproducibility

To study the reproducibility, two runs (3 and 8) were carried out under the same conditions (Table 1). Table 3 allows comparing the diameters d_{10} and d_{21} of the two runs. The d_{10} error is about ± 0.02 for an average value of 2.03 μm and the d_{21} error is about ± 0.13 for a mean value of 4.38 μm.

Influence of the Protocol Addition

According to the results obtained for the incorporation rate, the average diameters were determined only on blend samples resulting from the sequential protocol.

Influence of Mixing Time

Under the same operating conditions except for mixing time, a change of this later from 5 to 10 minutes (e.g. runs 3 and 10) causes a very small change of the average diameters (4.7% for d_{10} and 2.4% for d_{21} respectively). Therefore, the mixing time was considered to have no significant effect on the morphology of the PEG/PA system, which justified working with a mixing time of 5 min.

Influence of Filling Ratio

Similarly, if only the filling ratio changes from 0.7 to 0.8 (e.g. runs 1 and 11) a very small change of the average diameter is also observed (5.1% for d_{10} and 4.2% for d_{21}). Therefore, this change of the filling ratio change has no significant effect on the dispersed size of the PEG/PA system.

Influence of PEG Concentration

As shown in Figure 3, for different rotor speeds, the average diameters of the dispersed phase increase as the PEG concentration is increased. This observation can be related to the coalescence of the particles during the melt mixing. However, this increase remains relatively weak. Thomas and Groeninckx[6] made similar observations for the system ethylene propylene rubber (EPM)/nylon where the nylon (less viscous than EPM)) was the dispersed phase. The authors associated this result with the high viscosity of the matrix, which impeded the agglomeration of the dispersed phase: the matrix interlayer film drainage becomes more difficult and the coalescence decreases. In the case studied here, the viscosity difference between the components is so large that one can assume that coalescence is strongly reduced.

Influence of the Rotors Speed

Figure 3 shows that the average diameters decrease slightly when the rotors speed is increased. For most of the systems with a viscosity ratio ($0.01 \leq p \leq 20$), similar results were obtained showing that the phase size decreased[2] or remained practically unchanged[7] as the rotors speed and the shear rate increased.

Table 3.
Parameters useful for the model.

Experiment number	d_{10} (μm)	d_{21} (μm)	ϕ_d (actual value)	$\dot{\gamma}$ (s^{-1})	η_m (Pa.s)	η_b (Pa.s)	We^*	η^* ($\times 10^{-5}$)
1	1.18	1.68	0.009	79.1	205.8	186.6	5.06	2.20
2	1.74	3.02	0.092	79.1	205.8	76.1	1.91	5.39
3	2.05	4.51	0.184	79.1	205.8	28.8	0.50	14.2
4	2.8	5.83	0.174	59.4	208.3	31.7	0.59	12.9
5	1.56	2.65	0.010	39.6	211.9	189.9	3.38	2.16
6	2.13	4.17	0.091	39.6	211.9	79.2	1.23	5.18
7	2.86	6.36	0.181	39.6	211.9	29.6	0.36	13.9
8	2.01	4.25	0.182	79.1	205.8	28.2	0.47	14.5
9	–	–						
10	2.15	4.4						
11	1.12	1.61						

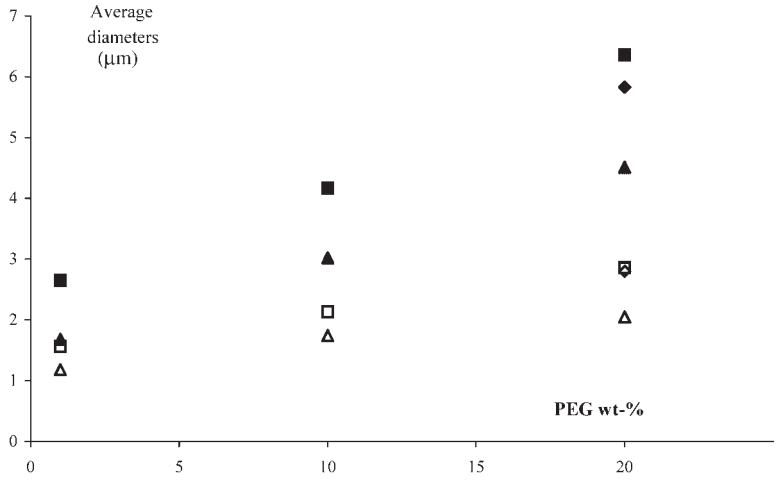

Figure 3.
Effect of PEG weight concentration on average diameters for different rotor speeds; △ = d_{10} for 200 rpm, ▲ = d_{21} for 200 rpm, ◇ = d_{10} for 150 rpm, ◆ = d_{21} for 150 rpm, □ = d_{10} for 100 rpm, ■ = d_{21} for 100 rpm.

Dependence of the Dispersed Phase Size on the Processing Parameters

To study the influence of the processing parameters on the particle size, the modified Weber number We*: $\left(\mathrm{We}* = \frac{\dot{\gamma} d \eta_b \left[1-(4\phi_m\phi_d)^{0.8}\right]}{\gamma}\right)$ was studied versus the *ratio* $\left(\eta* = \left(\frac{\eta_d}{\eta_b}\right)\right)$.

Table 3 reports the values of We* and η* together with:

(i) the actual volume fraction ϕ_d and ϕ_m of the two components, calculated using the value of the incorporation rate,

(ii) the shear rate in the mixing chamber, $\dot{\gamma}$, determined according to equation (10),

(iii) the blend viscosity, η_b, estimated through the log-linear mixing rule generally recommended for polymer blends when the viscosities of the components are very different[8]:

$$\log(\eta_b) = \phi_d \log(\eta_d) + \phi_m \log(\eta_m) \tag{12}$$

(iv) the surface tension and the polar and dispersive contributions at 275 °C, obtained from values reported[9] for other temperatures by using the temperature coefficient $(\frac{d\gamma}{dT})$ and the polarity $(x^p = \frac{\gamma_p}{\gamma})$

$$\gamma = \gamma_1 + \gamma_2 - 4\frac{\gamma_{1p}\gamma_{2p}}{\gamma_{1p}+\gamma_{2p}} - 4\frac{\gamma_{1d}\gamma_{2d}}{\gamma_{1d}+\gamma_{2d}} \tag{13}$$

where γ is the interfacial tension between component 1 and component 2, γ_i is the surface tension of component i, γ_{ip} and γ_{id} are the polar and the dispersive fraction of the surface tension of component i, respectively. The surface tension and the polar and dispersive contributions at 275 °C, obtained from values reported[10] for other temperatures by using the temperature coefficient $(\frac{d\gamma}{dT})$ and the polarity $(x^p = \frac{\gamma_p}{\gamma})$. Finally, according to equation (13), the resulting interfacial tension between PA and PEG is 3.2 mN/m.

The coefficients of the power law were determined by modeling the logarithm of $We*$ for each experiment with:

$$\ln(We_i^*) = \theta_0 + \theta_1 \ln(\eta_i^*) + \varepsilon_i \tag{14}$$

where θ_0 and θ_1 are coefficients and ε_i is the unknown experimental error

This leads to a system of equations represented in the following matrix form:

$$Y = X\theta + \varepsilon \tag{15}$$

Table 4.
Confidence intervals of the We^* model coefficients with a risk of 10%.

Coefficient	Estimated value	$\hat{\theta}^{red}_{min}$	$\hat{\theta}^{red}_{max}$
ϕ_0	−13.76	−14.30	−13.21
ϕ_1	−1.44	−1.49	−1.38

where Y is the vector of experimental values of $\ln(We_i^*)$, θ the vector of the model coefficients and ε the vector of the experimental errors. X is the model matrix obtained from the experiments realized and the model chosen.

The model coefficients were calculated using a multi-linear regression (Nobelen and al.[10]). Four experiments (runs 1, 2, 6 and 7) were used to identify the model parameters, two experiments (runs 4 and 5) for the validation of the model and two experiments (runs 3 and 8) for duplication.

Table 4 gives the results with a 90% reduced confidence interval $\left[\hat{\theta}^{red}_{min}; \hat{\theta}^{red}_{max}\right]$ for each estimated value of the coefficients. This confidence interval was determined by using the identification variance, σ_i^2. The number of degrees of freedom, NDF, for the identification experiments, ν_I, is given by the difference between the number of runs and the number of the coefficients of the model. Thus, $\nu_i, = 2$ (4 runs less 2 model coefficients). The variance σ_i^2 was obtained by dividing the sum of squared deviations between experimental and the model values of $\ln(We_i^*)$ by NDF ν_I. Its value is σ_i^2 is 0.065. Confidence intervals were used to determine if the coefficients values are significantly different from zero. In fact, the uncertainty on the estimated coefficients is all the more important that the interval is centred on zero. In our case, none of the coefficients needed to be rejected.

Fischer-Snedecor's test was then applied to the present model. This test is based on the ratio of the error variances. The validation of the model with a risk of 10% implies the verification of the following relationship:

$$\frac{1}{F_{0.05}(\upsilon_j, \upsilon_i)} \leq \frac{\sigma_i^2}{\sigma_j^2} \leq F_{0.05}(\upsilon_i, \upsilon_j) \tag{16}$$

where σ_k^2 is the error variance and $F_{0.05}(\upsilon_i, \upsilon_j)$ is the Fischer-Snedecor's value with a probability of 5% and with the degrees of freedom υ_i and υ_j. The results are presented in Table 5.

For validation experiments, the NDF, ν_v, is 2 (2 runs). The validation variance, σ_v^2, obtained by dividing the sum of square deviations between experimental and model values of $\ln(We_i^*)$ by the NDF ν_v, is equal to 0.17. For duplication experiments, since the mean value of $\ln(We_i^*)$ was used to calculate the sum of squares, the NDF ν_r, is 1 (2 runs minus 1 mean value). The duplication variance, σ_r^2, was obtained by dividing the sum of square deviations between experimental data and the mean value of $\ln(We_i^*)$, by the NDF ν_r. So $\sigma_r^2 = 0.0015$. The ratios of the variances respect Fischer-Snedecor's condition, which validates the model which can be written as:

$$We^* = 1.06 \times 10^{-6}(\eta*)^{-1.44} \tag{17}$$

Figure 4 shows the evolution of the experimental values of We^* versus η^*. The full line represents We^* calculated with the model and the two dotted lines correspond to the confidence interval at 10%. All the experiments are within this interval showing that the power law fits well the measured data.

Table 5.
Fischer – Snedecor's test applied to the model.

Variance ratio	$F = \sigma_i^2/\sigma_j^2$	(ν_i, ν_j)	$1/F_{0.05}(\nu_j, \nu_i)$	$F_{0.005}(\nu_i, \nu_j)$
Identification/Duplication	44.64	2; 1	0.05	199.50
Validation/Identification	2.65	2; 2	0.05	19.00
Validation/Duplication	118.15	2; 1	0.05	199.50

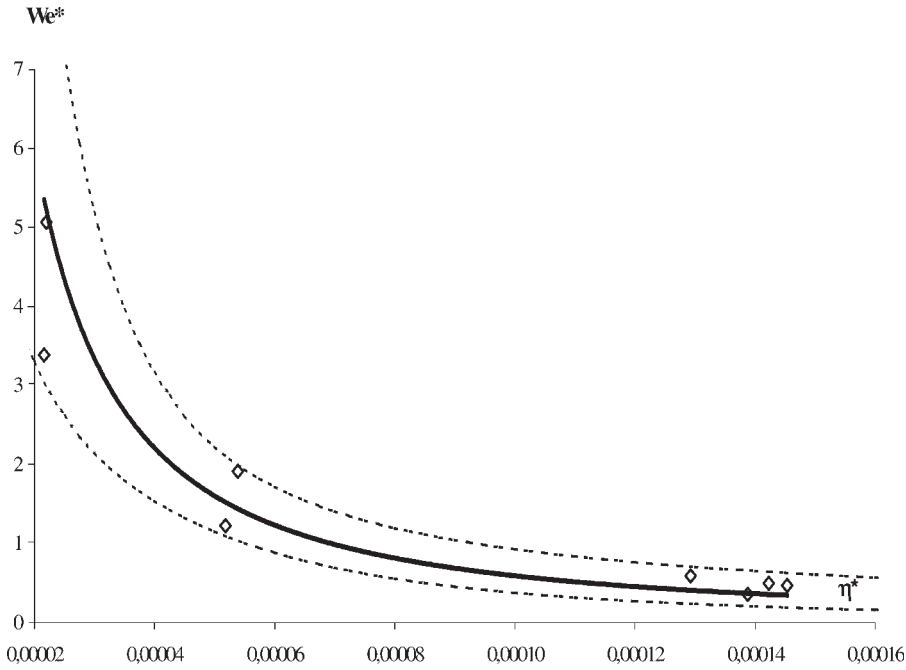

Figure 4.
We* versus η^*.

Conclusion

The morphology of PEG/PA blends with an extremely low viscosity ratio has been investigated in this study. A mixing protocol in a Haake internal mixer has been validated. For this system, it appears that a sequential addition, with a filling ratio between 0.7 and 0.8 and a mixing time of 5 minutes provides reproducible dispersed phase size with a good incorporation rate of the PEG into the PA matrix. The influence of the rotors speed and PEG concentration on the morphology showed similar trends already observed for some other systems with viscosity ratios between 0.01 and 20. The dispersed phase size decreases by increasing the rotors speed and by decreasing the PEG concentration. However, these effects stay limited: this can be related to the high viscosity of the matrix, which reduce the probability of coalescence during the melt mixing. Interfacial tension, concentration, shear rate and viscosity ratio were correlated to the observed phase size through a relationship similar to that obtained by Serpe and al.[2]

Acknowledgements: The authors are grateful to Drs. J.M. Pujol, P. Pitiot and P. Hervé (Rhodia Recherches & Technologies -St Fons, France-) for their very fruitful cooperation during this work.

[1] S. Wu, *Polym. Eng. Sci.* **1987**, *27*, 335.
[2] G. Serpe, J. Jarrin, F. Dawans, *Polym. Eng. Sci.* **1990**, *30*, 553.
[3] J. E. Goodrich, R. S. Porter, *Polym. Eng. Sci.* **1967**, *7*, 45.
[4] M. Bousmina, A. Ait-Kaidi, J. B. Faisant, *The society of rheology* **1999**, *43*, 415.
[5] A. Ait-Kadi, P. Marchal, A. S. Chrissemant, M. Bousmina, L. Choplin, *Can. J. Chem. Eng.* **2002**, *80*, 1166.
[6] S. Thomas, G. Groeninckx, *Polymer* **1990**, *40*, 5799.
[7] B. D. Favis, *J. Appl. Polym. Sci.* **1990**, *39*, 285.
[8] N. Grizzuti, B. Giovanna, G. Iorio, *The society of Rheology* **2000**, *44*, 149.
[9] S. Wu, in: "*Polymer Handbook*", 3rd ed., J. Brandup, E. H. Immergut, Eds., J. Wiley & Sons, New York, **1989**, p. VI/411ff.
[10] M. Nobelen, S. Hoppe, C. Fonteix, F. Pla, M. Dupire, B. Jacques, *Chem. Eng. Sci.* **2006**, *61*, 5334.

